Host−Guest Interactions and Crystalline Structure Evolution in Clathrate Phases Formed by Syndiotactic Polystyrene and 1,2-Dichloroethane: A Two-Dimensional FTIR Spectroscopy Investigation

Pellegrino Musto,[†,*] Paola Rizzo,[‡] and Gaetano Guerra[‡]

Institute of Chemistry and Technology of Polymers (ICTP), National Research Council of Italy, via Campi Flegrei, 34, Olivetti Building, 80078 Pozzuoli (NA), Italy, and Dipartimento di Chimica, Università di Salerno, via S. Allende, 84081 Baronissi (SA), Italy

Received October 27, 2004; Revised Manuscript Received May 2, 2005

ABSTRACT: 2D correlation spectroscopy has been used to investigate the behavior of a clathrate sample of syndiotactic polystyrene including 1,2-dichloroethane (DCE) in the crystalline phase. Isothermal desorption of DCE at 80 °C was selected as the perturbation process, with time as external variable, and it was shown that the response function of the system was an exponential decay. The resolution enhancement brought about by 2D analysis and the possibility to identify the temporal relationship among asynchronously correlated events allowed us to gather information on host−guest molecular interactions and on the development of the crystal structure, not readily available with more conventional approaches. It was shown that a characteristic peak of the guest molecules, i.e., the CH_2 wagging mode of the trans conformer at 1235 cm^{-1}, is significantly influenced by host−guest interactions taking place within the cavity of the s-PS clathrate. It was confirmed that the desorption of the guest molecules initially present in the amorphous phase of the sample takes place at a faster rate than the desorption of those included into the cavities of the crystalline phase. This effect, in turn, allowed us to discriminate between the peaks of DCE absorbed in the two phases. In terms of dynamic behavior, it was found that DCE peaks respond faster to the applied perturbation than the polymer peaks, and as for the polymer spectrum, the crystalline phase responds faster than the amorphous phase. The latter effect has been tentatively attributed to the occurrence of a mesomorphic phase.

Introduction

Syndiotactic polystyrene (s-PS) is characterized by a complex polymorphic behavior, with four crystalline forms denoted α, β, γ, and δ.[1,2] The first two forms, α and β have the chains in the trans-planar zigzag conformation with identity period of 5.1 Å, while the γ and δ forms display a helical s(2/1)2 chain conformation with an identity period of 7.7 Å.[3−8] Besides the four crystalline forms, two mesomorphic forms of s-PS, containing chains in the trans planar[9−11] and **s**(2/1)2 helical conformations[12] have been described.

Of the various s-PS crystalline modifications, the most interesting is certainly the δ form,[13−14] in that, by only minor rearrangements, it can form clathrate structures with suitable low- molecular weight compounds.[15−17] Thus, unlike conventional semicrystalline polymers, this material is able to absorb penetrant molecules not only in the amorphous phase but also in the crystalline phase. Moreover, by removing the guest molecules from the clathrate phase by suitable solvent treatments, the emptied clathrate δ form can be obtained. Sorption studies have demonstrated that this thermoplastic material can readily absorb several halogenated or aromatic hydrocarbons even when they are present in trace amounts in water or in the atmosphere. These studies suggested that this material might be promising for chemical separation purposes as well as for water and air purification.[18−19] More recently, thin films of s-PS in the δ form have been proposed as elements for molecular sensors.[20]

It is clear from the preceding discussion that the guest diffusion behavior of the s-PS clathrate form is very relevant from both a fundamental and a technological perspective. However, a complete characterization of the material in this respect is not straightforward. First of all the s-PS clathrate is a two-component system comprising an amorphous fraction (usually around 50%) and a crystalline phase, whose transport behaviors are largely different. It is very difficult or even impossible to investigate the system without a tool that is able to discriminate between the guest molecules present in the two phases. Furthermore, it has been shown that sorption and desorption processes are often accompanied by structural rearrangements of the polymeric substrate, with the consequence that the polymeric host is to be considered by itself a dynamically evolving system rather than a static structure.[21,22] A technique capable of providing information at the molecular level and of probing the local environment of both the guest molecules and the polymeric host is therefore needed to fully characterize these complex systems. In this respect, FTIR spectroscopy has proven to be particularly well suited, offering the additional advantages of fast sampling rate, high sensitivity, and accurate quantification. In fact, numerous studies have appeared in the literature in which various aspects of the behavior of s-PS clathrates have been thoroughly investigated by FTIR measurements.[23a−n] Limitations which often preclude attainment of molecular level information contained in the vibrational spectrum are lack of resolution and/or the occurrence of very subtle effects which represent a

* Corresponding author. E-mail address: musto@irtemp.na.cnr.it.
† National Research Council of Italy.
‡ Università di Salerno.

10.1021/ma0477899 CCC: $30.25
Published on Web 06/11/2005

challenge for the detection limits of the technique and can hardly be investigated in a systematic fashion.

In connection with these problems, a new methodology has been recently introduced, known as two-dimensional infrared (2D-IR) correlation spectroscopy.[24a−c] This approach, originally developed for the study of transient (time-resolved) signals, is receiving considerable attention as a powerful tool to be employed as an aid in the interpretation of complex, multiply overlapped spectra, such as those generally encountered in condensed state systems. 2D-IR spectroscopy offers a number of distinct advantages which can be summarized as follows: (i) the capability of improving the resolution, thus revealing otherwise undetectable components; (ii) the possibility to provide information about inter- and intramolecular interactions by selective correlation of peaks; (iii) the possibility to establish the relative rate of change of the different events taking place in a transient process, making use of asynchronous spectral information. In the present contribution the transmission spectra gathered during the desorption of 1,2-dichloroethane (DCE) from an s-PS clathrate film are analyzed by means of 2D-IR correlation spectroscopy. As will be shown in the following sections, all of the above advantages of the methodology are very relevant to improving the interpretation of the spectral response of the system under investigation.

Background

The theory of 2D-IR spectroscopy was originally developed by Noda[24a−c] in connection with dynamic rheooptical data. In essence, it is a perturbation-based spectroscopy in which a system, initially at equilibrium, is subjected to the action of an external perturbing force, and its response in terms of spectroscopic signal variations is analyzed. Typical spectroscopic responses to external stimuli comprise changes in peak intensities, positions and directional absorbances (dichroic effects). Initially, the 2D-IR approach was developed for the specific case of perturbation functions having simple sinusoidal form with fixed frequency. Soon after, it was realized that the particular excitation waveform does not alter the basic principles of the analysis, and more recently, Noda introduced a generalized formalism which can be applied, in principle, to any excitation waveform.[24d]

Since a number of controversial issues still persist about the application of 2D-IR spectroscopy and the interpretation of synchronous and asynchronous spectra,[25−27] it seems useful to briefly review the underlying principles, with special emphasis on the aspects of the theory that are more relevant to the present application. On completely general grounds, the 2D-IR methodology is a correlation analysis by which one measures the *covariance* of two variables (in the case at hand, spectral intensities) as they evolve as a function of a third common variable related to the perturbing function (time, in the present case).

Formally, if we consider a time-dependent spectral intensity, $y(\nu,t)$ observed for a period between $-T/2$ and $T/2$, we may define a dynamic spectrum $\tilde{y}(\nu,t)$ as

$$\tilde{y}(\nu,t) = \begin{cases} y(\nu,t) - \bar{y}(\nu) & \text{for } -T/2 \le t \le T/2 \\ 0 & \text{otherwise} \end{cases} \quad (1)$$

In eq 1 $\bar{y}(\nu)$ represents the reference spectrum and serves the purpose of eliminating the static contribution from the signal. It can be selected in a number of ways depending on the specific excitation waveform. For nonperiodic perturbing functions it has been shown that the most convenient reference spectrum to use is the *static* or *time-averaged* spectrum, defined as

$$\bar{y}(v) = \frac{1}{T}\int_{-T/2}^{T/2} y(\nu,t)\, \mathrm{d}t \quad (2)$$

The complex cross-correlation intensity between dynamic spectral intensities at wavenumbers ν_1 and ν_2 is

$$\Phi(\nu_1,\nu_2) + i\Psi(\nu_1,\nu_2) = \frac{1}{\pi T}\int_0^\infty \tilde{Y}(\nu_1,\omega)\cdot\tilde{Y}^*(\nu_2,\omega)\, \mathrm{d}\omega \quad (3)$$

In the above equation $\tilde{Y}_1(\omega)$ represents the forward Fourier transform (FT) of the dynamic spectral intensity $\tilde{y}(\nu_1,t)$, i.e.

$$\tilde{Y}(\nu_1,\omega) = \int_{-\infty}^{\infty} \tilde{y}(\nu_1,t)\mathrm{e}^{-i\omega t}\, \mathrm{d}t \quad (4)$$

while $\tilde{Y}_2^*(\nu_2,t)$ is the conjugate of the FT of the dynamic spectral intensity $\tilde{y}(\nu_2,t)$, that is

$$\tilde{Y}_2^*(\nu_2,t) = \int_{-\infty}^{\infty} \tilde{y}(\nu_2,t)\mathrm{e}^{i\omega t}\, \mathrm{d}t \quad (5)$$

The correlation spectrum (eq 3) actually determines the degree of linear dependence between two variables.[28] Thus, if the intensities at two different wavenumbers change linearly with the chosen variable, a synchronous spectrum will be obtained, and the asynchronous spectrum will be zero (it will only display noise). Conversely, an asynchronous peak will be produced in two instances: (i) the two intensity changes are otherwise completely unrelated; (ii) they are related in a nonlinear fashion. In dealing with real systems, a complete absence of relationship can be neglected as random noise fluctuations. Furthermore, if the response function has a well-defined form, it is possible to directly derive the expression for the corresponding 2D correlation spectrum in a closed analytical form. This will provide further insight into the significance of the linear and nonlinear correlations between the variables, as revealed by 2D analysis. A response function often encountered in reaction kinetics and in mass transport phenomena is the exponential decay, which can be suitably applied to describe the behavior of the system under investigation, as demonstrated by the data in Figure 1, which shows the time evolution of a well resolved DCE peak at 1234 cm^{-1}. In this respect, it is worth noting that the kinetic profile of the DCE peak is closely simulated by a biexponential decay function with residual, of the form

$$y = A_1\cdot\mathrm{e}^{-k_1 t} + A_2\mathrm{e}^{-k_2 t} + B \quad (6)$$

while a monoexponential decay function gives a very poor fit. In close agreement with this observation, it will be shown in the following sections that the 1234 cm^{-1} peak is in fact the sum of two distinct components decaying at substantially different rates.

For response functions of this type, the dynamic spectrum at wavenumber ν can be expressed as

$$y(\nu,t) = \begin{cases} \tilde{y}(\nu,t) = A(\nu)\mathrm{e}^{-k(\nu)t} & \text{for } t \ge 0 \\ 0 & \text{otherwise} \end{cases} \quad (7)$$

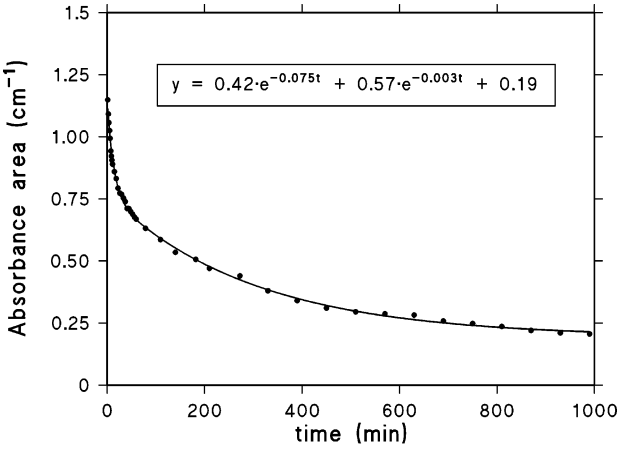

Figure 1. Absorbance area of the DCE peak at 1234 cm^{-1} as a function of time for the desorption measurement carried out at 80 °C on a film of s-PS in clathrate form. The solid circles indicate the experimental data, the solid line corresponds to the simulation of the kinetic model (biexponential decay with residual).

where $A(\nu)$ and $k(\nu)$ are the coefficient of the decay process and the characteristic rate constant, respectively. To determine the complex cross-correlation function, we consider two spectral intensities at frequencies ν_1 and ν_2, having different values of A and k. Evaluating the Fourier transform, $\tilde{Y}(\nu_1,\omega)$ and the complex conjugate Fourier transform, $\tilde{Y}^*(\nu_2,\omega)$ of these dynamic spectral intensities, and substituting in eq 3, one obtains[29]

$$\Phi(\nu_1,\nu_2) = \frac{A(\nu_1)\cdot A(\nu_2)}{T} \cdot \frac{1}{k(\nu_1) + k(\nu_2)} \qquad (8)$$

$$\Psi(\nu_1,\nu_2) = \frac{A(\nu_1)\cdot A(\nu_2)}{\pi T} \cdot \frac{\ln k(\nu_2) - \ln k(\nu_1)}{k(\nu_1) + k(\nu_2)} \qquad (9)$$

Equations 8 and 9 clarify the meaning of the synchronous and asynchronous spectra. In the synchronous spectrum a peak will appear at coordinates (ν_1,ν_2) whenever there are two peaks located at ν_1 and ν_2 undergoing intensity changes during the sampling interval, irrespective of their rate constants. The *synchronous* spectrum is symmetric [i.e. $\Phi(\nu_1,\nu_2) = \Phi(\nu_2,\nu_1)$] and consists of *autopeaks* located along the main diagonal (i.e., at coordinates ν_i, ν_i) and *cross-peaks* appearing at off-diagonal positions. The *autopeaks* identify the signals that undergo changes during the experiment. They are always positive and their intensity can be considered as a measure of the susceptibility of the relative signals to the external stimulus.[30−31] The *cross-peaks,* on the other hand, are positive if the two signals change in the same direction (they both increase or decrease) and are negative otherwise.

Conversely, the *asynchronous* correlation spectrum identifies decay processes having different rates as a result of the term $\ln k(\nu_2) - \ln k(\nu_1)$, which assumes nonzero values only if the rate constants for the decay processes at the two wavenumbers are different. Therefore, it contains no *autopeaks* but only *cross-peaks* at off-diagonal positions. The *asynchronous* spectrum is antisymmetric [i.e. $\psi(\nu_1,\nu_2) = -\psi(\nu_2,\nu_1)$]; a cross-peak at coordinates (ν_1,ν_2) is positive if the intensity change at ν_1 is accelerated with respect to that at ν_2 and is negative otherwise. However, this rule is reversed if $\Phi(\nu_1,\nu_2) < 0$.[29−31] A direct comparison between the *synchronous* and *asynchronous* spectra is also informative. Recalling that any two intensities changing simultaneously with time will produce a synchronous peak while only those changing at different rates will give rise to an asynchronous peak, a synchronous peak at (ν_1,ν_2) having no counterpart in the asynchronous spectrum, indicates that the decay processes at the corresponding frequencies are occurring at the same rate.

Experimental Part

Materials and Preparation Procedures. s-PS was synthesized using a homogeneous catalyst consisting of $CpTiCl_3$ and methylalumoxane (MAO) in toluene, according to the method described in the literature.[32] The polymer fraction insoluble in acetone was 92%. The intrinsic viscosity of the acetone insoluble fraction, determined in tetrahydronaphthalene at 135 °C with an Ubbelhode viscometer, was 0.6 dL/g.

Film samples in δ form were obtained by casting a 5.0 wt % solution of s-PS in chloroform at room temperature, followed by treatment with boiling acetone for 5 h and desiccation at 60 °C for 2 h to remove acetone. DCE sorption, leading to clathrate films was achieved by immersing δ-form samples for 4 h in a 0.5 wt % aqueous solution of DCE. The first spectrum was taken after 60 min of desorption at 80 °C, in these conditions the total DCE content, as measured by FTIR spectroscopy was 2.70 wt %; of which 2.56 wt % in the trans conformation and 0.14 wt % in the gauche conformation, corresponding to an X_t value (molar fraction of trans conformer) of 0.95.[23l,n]

DCE desorption measurements were performed in a vacuum tight environmental chamber directly fitted in FTIR spectrometer. This apparatus was constructed in the house by modifying the commercially available SPECAC 20100 cell. Temperature control was achieved by an Eurotherm PID temperature regulator mod. 2416 with an accuracy of (±0.5 °C). All measurements were carried out at 80 °C under a continuous flux of dry nitrogen (60 cm^3/min).

FTIR Spectroscopy. Transmission FTIR spectra were obtained using a System 2000 spectrometer from Perkin-Elmer (Norwalk, CT). This instrument employs a germanium/KBr beam splitter and a wide-band deuterated tryglycine sulfate (DTGS) detector. The instrumental parameters adopted for the spectral collection were as follows: resolution 4 cm^{-1}, optical path difference (OPD) velocity = 0.20 cm s^{-1}, and spectral range 4000−400 cm^{-1}. A single data collection was performed for each spectrum (3601 data points) which, under the selected instrumental conditions, took 6 s to complete. It was found that, even with a single acquisition, the signal-to-noise ratio of the spectra (5000:1) was suitable for 2D-IR analysis. Spectra were collected at time intervals increasing as the desorption process slowed, getting closer to equilibrium. A typical kinetic test lasted 1200 min and spectral collection was triggered every 80 s in the first 15 min, every 5 min up to 60 min, every 30 min up to 330 min, and every 60 min afterward. A dedicated software package for the acquisition of time-resolved infrared spectra was used to drive the FTIR spectrometer during the test (Timebase V. 1.1 from Perkin-Elmer).

2D-IR Correlation Analysis. Before performing cross-correlation analysis, the experimental spectra were preprocessed to avoid the occurrence of artifacts due to baseline instabilities and other nonselective effects.[33,34] The frequency regions of interest (1130−1305, 995−820, and 595−480 cm^{-1}) were truncated and were subjected to a linear baseline correction, followed by offset to the zero absorbance value. Generalized 2D-IR analysis was performed by a computer program written in house in the Grams/32 environment (Galactic Industries Co., Salem, NH), using the associated programming language Array Basic. A recently developed algorithm was employed, relying on the Hilbert transform,[35] which offers an easier and more efficient method for the numerical evaluation of the correlation intensities.

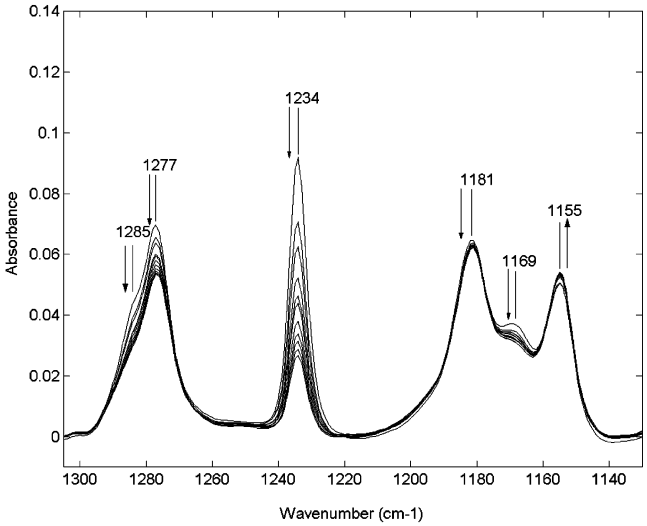

Figure 2. Transmission FTIR spectra in the wavenumber range 1130−1305 cm^{-1}, collected every 120 min, from 60 to 1200 min, during the isothermal desorption experiment at 80 °C. The arrow's direction indicate absorbance increase or decrease of the corresponding peaks.

The 2-D correlation analysis was performed on an evenly spaced sequence of 20 spectra collected at a constant sampling interval of 60 min. It was found that, considering shorter time intervals does not improve the quality and resolution of the resulting correlation spectra.

The notation adopted to identify the peaks appearing in the correlation spectra is the following: the *x*-axis frequency coordinate is written first, followed by the *y*-axis coordinate, both enclosed in square brackets. Following the coordinate values, a ± sign enclosed in round brackets specifies the positive or negative value of the peak. The sign is omitted for *autopeaks*, these being always positive. It is explicitly noted that, for concision, only the peaks appearing in the lower side of the spectrum with respect to the diagonal line with coordinates $[\nu_i,\nu_i]$ are referred to, with the understanding that, due to the symmetry of the correlation spectra, corresponding cross-peaks are located in the upper side of the spectrum, at appropriate positions.

Results and Discussion

1305−1130 cm^{-1} Interval. In the present contribution attention is focused on the three regions of the infrared spectrum that are the most influenced by DCE desorption, namely the 1305−1130, 995−820, and 595−480 cm^{-1} wavenumber ranges.

In particular, in Figure 2 are displayed the FTIR transmission spectra in the 1305−1130 cm^{-1} interval, collected at different times during the isothermal desorption experiment at 80 °C. The most relevant features are associated with the peaks of DCE at 1285 cm^{-1} (CH_2 wagging for the gauche conformer, ν_{14}, symmetry species B)[36a,b] and at 1234 cm^{-1} (CH_2 wagging for the trans conformer, ν_{16}, symmetry species B_u).[36a,b] Both these peaks steadily decrease with time.

In the present interval the s-PS spectrum displays several bands: at 1277 cm^{-1} is observed a complex mode with multiple contributions (mostly C−C plus C−C′ stretching, where the apex denotes a chain carbon).[37a,b] A peak at 1181 cm^{-1} has contributions from aromatic C−H in-plane bending (78% PED) and C−C′ stretching (10% PED). The 1155 cm^{-1} mode is again highly coupled, with contributions from C′C′H bending (73% + 19% PED) and C′−C′ stetching (14% PED).[37a] Finally, the component at 1169 cm^{-1} has been tentatively assigned to the combination of the fundamentals 547.7 + 621.1 = 1168.8 cm^{-1}.[37b]

It is found that the above peaks of s-PS are all affected, albeit to a lower extent in comparison to those of DCE. This is an indication that the desorption of guest molecules and/or the thermal treatment induce structural modifications in the polymer substrate.

The synchronous cross-correlation spectrum obtained from the data of Figure 2 is displayed in Figure 3A. Here two autopeaks are evident at [1234, 1234 cm^{-1}] and at [1285, 1285 cm^{-1}] corresponding to the spectral features that are changing to the larger extent. The autopeak at higher frequency displays a well-defined shoulder at 1277 cm^{-1} which is not resolved from the main component. Several cross-peaks are identified in the synchronous spectrum, the most intense appearing as a distinct doublet at [1277, 1234 (+) cm^{-1}] and [1285, 1234 (+) cm^{-1}].

The positive sign of the cross-peaks reflects the circumstance that the corresponding signals are changing in the same direction (they both decrease). The negative cross-peak at [1234, 1154 (−) cm^{-1}] indicates that the 1154 cm^{-1} signal is the sole increasing feature.

It is worth noting that the synchronous spectrum of Figure 3A presents several cross-peaks at [1234, 1154 (−) cm^{-1}], [1234, 1168 (+) cm^{-1}], and [1234, 1185 (+) cm^{-1}] although the corresponding autopeaks are not apparent. This is due to the much lower intensity of these autopeaks with respect to the ones at [1234, 1234 cm^{-1}] and [1285, 1285 cm^{-1}]. The synchronous cross-correlation spectrum relative to the peaks of the s-PS (1130−1220 cm^{-1} range) was therefore analyzed by use of a lower intensity scale (see Figure 3B) which clearly evidences all the autopeaks along with their correlation counterparts. Again, the cross-peaks involving the 1154 cm^{-1} signal are both negative, confirming that the latter is the only increasing feature. Since it has been shown that the desorption process tends to reduce the overall structural order,[21] the above results suggest that the 1154 cm^{-1} peak is prevailingly associated with the amorphous phase while the peaks at 1168 and 1277 cm^{-1} arise from the crystalline phase. With respect to the feature at 1185, it is noted that the spectrum of the amorphous sample (not shown) displays a symmetric peak located at 1181 cm^{-1}, while in the semicrystalline samples this peak increases in intensity and displays a shoulder at higher wavenumbers. The above evidence points to the occurrence of a crystalline component at 1185 cm^{-1} superimposed on the peak at 1181 cm^{-1}.

In Figure 4 is reported the asynchronous cross-correlation spectrum in the 1130−1305 cm^{-1} range calculated from the spectra of Figure 2, which clearly demonstrates the resolution enhancement brought about by spreading the spectrum over the second frequency domain. The most striking feature of the asynchronous spectrum is represented by a cross-correlation peak at [1235, 1231 (−) cm^{-1}] which reveals that the CH_2 wagging vibration of DCE in the trans conformation is actually the sum of two distinct components. This effect goes completely undetected in the conventional absorbance-frequency spectrum, when the data are collected at a nominal resolution of 4 cm^{-1} (see Figure 2 and Figure 5, upper trace). The negative sign of the cross-correlation peaks implies a faster decay rate of the 1231 cm^{-1} component as compared to the 1235 cm^{-1} feature. Closely related to the above feature, for interpretative purposes, is the intense asynchronous peak located at

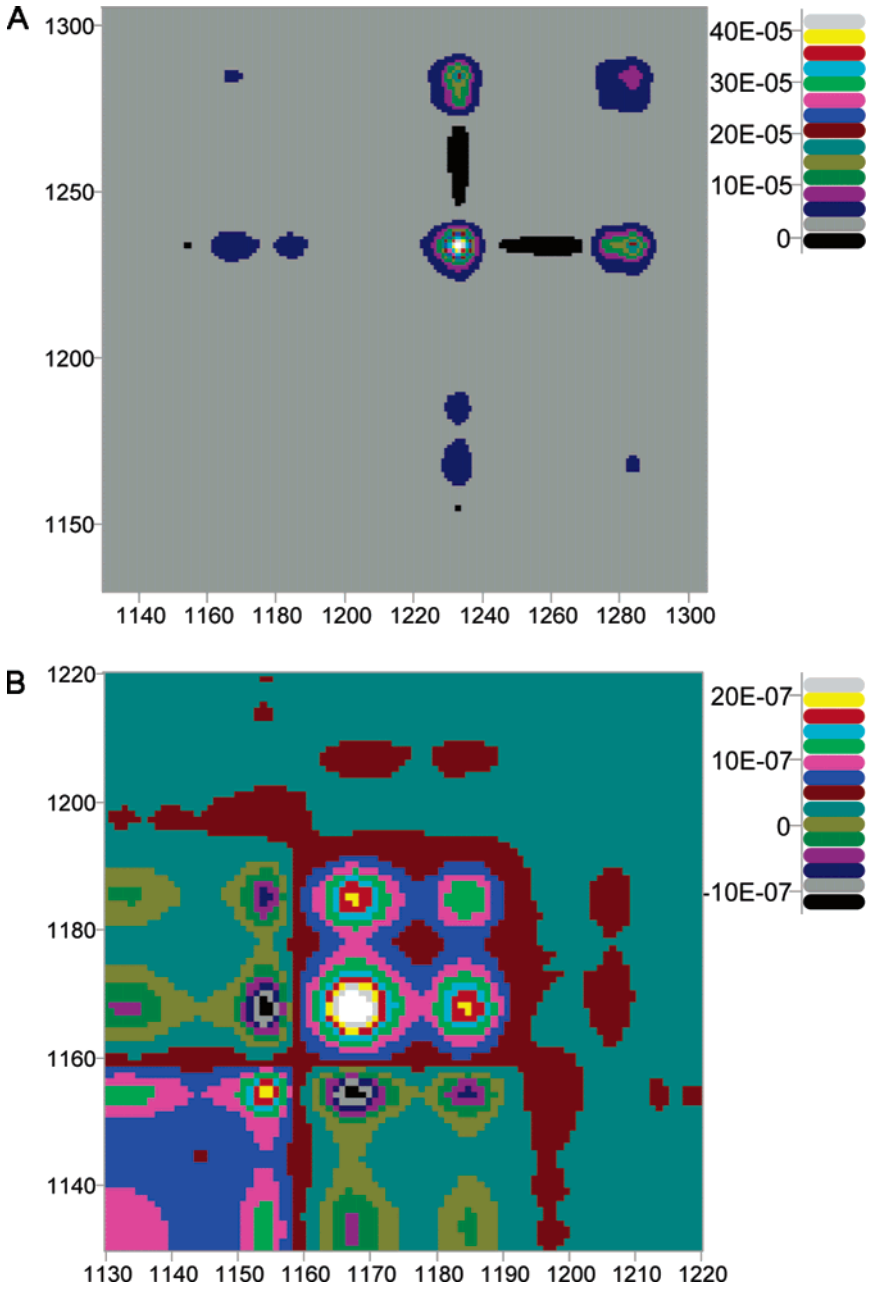

Figure 3. Synchronous 2D correlation spectrum in the wavenumber range 1130−1305 cm^{-1} (A) and in the wavenumber range 1130−1220 cm^{-1} (B).

[1285, 1235 (+) cm^{-1}], which indicates that the trans and gauche conformers of DCE are desorbed at different rates, with that of the gauche conformer being higher. Also of interest is the absence of asynchronous correlation at [1285, 1231 cm^{-1}].

An explanation of the above observations can be put forward on the basis of the conformational selectivity of the clathrate phase evidenced in previous studies by conventional 1D analysis.[23l,n,38] Thus, in the crystalline nanocavities the *trans* conformer of DCE is largely prevalent, while in the amorphous phase both conformers coexist at equilibrium, with a population ratio close to 50:50. Low intensity molecular interactions which are established between the guest molecules and the host lattice within the crystalline cavities are likely to induce a subtle shift of the CH_2 wag mode of trans DCE. Therefore, the two component structure of the 1234 cm^{-1} peak is likely due to the trans conformer being present in the amorphous region and in the cavities of the crystalline phase.

From the temporal relationship between the 1285 and the 1235 cm^{-1} components, confirmed by previous studies,[23l,n,38], it emerges that the desorption rate of DCE from the amorphous phase is faster than that from the crystalline phase. Thus, the slower decay rate of the 1235 cm^{-1} feature with respect to the one at 1231 cm^{-1} allows us to assign the high-frequency component to DCE in the crystalline lattice and the low-frequency component to the DCE in the amorphous phase. The absence of asynchronous correlation at [1285, 1231 cm^{-1}] reflects the simultaneous desorption of the two DCE conformers from the amorphous phase.

The above interpretation has been confirmed by collecting the spectra with polarized radiation at higher resolution (0.5 cm^{-1}) on an axially oriented s-PS film containing DCE (Figure 5). The two component struc-

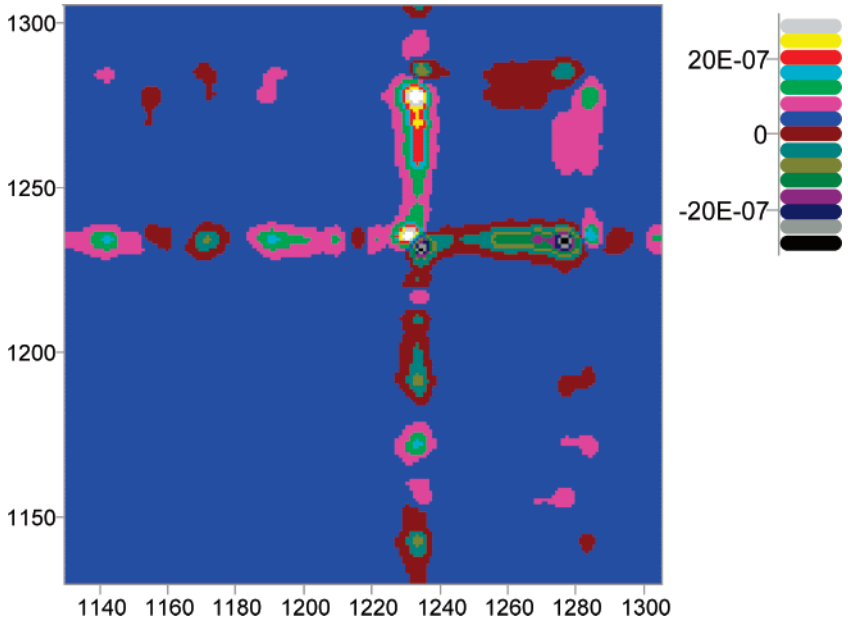

Figure 4. Asynchronous 2D correlation spectrum in the wavenumber range 1130−1305 cm^{-1}.

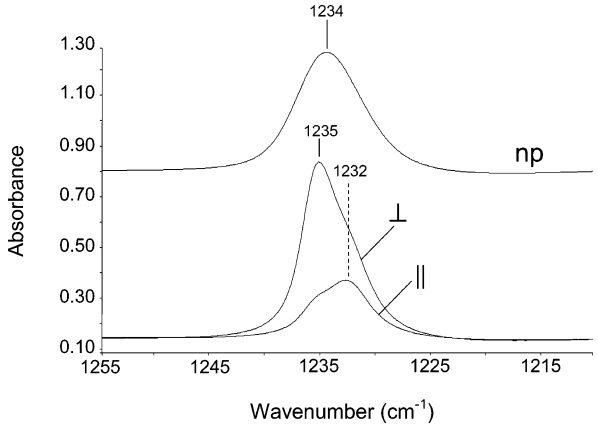

Figure 5. FTIR spectrum for the wavenumber range 1255−1215 cm^{-1}, collected at resolution of 0.5 cm^{-1} with the polarization plane parallel (||) and perpendicular (⊥) to the draw direction, for an uniaxially oriented film ($\lambda \approx 3$) including the s-PS/DCE clathrate phase. The FTIR spectrum of the same uniaxially oriented film collected with unpolarized light and at resolution of 4 cm^{-1} (*np*) is also reported for comparison.

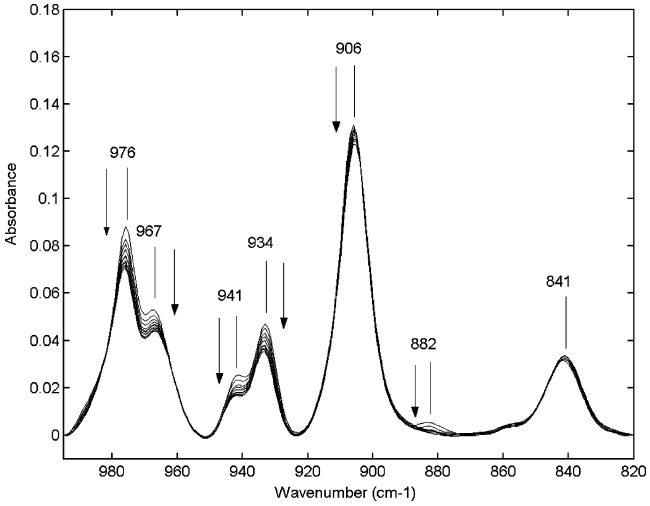

Figure 6. Transmission FTIR spectra in the wavenumber range 995−820 cm^{-1}, collected every 120 min, from 60 to 1200 min, during the isothermal desorption experiment at 80 °C. The arrow's direction indicates absorbance increase or decrease of the corresponding peaks.

ture of the band emerges clearly in the high-resolution measurements, which also show a strong dichroic character of the high-frequency peak. Since it is known that the DCE trans conformer included into the axially oriented clathrate phase presents some degree of order with respect to the draw direction,[39] while the DCE included in the amorphous region remains essentially unoriented, the dichroic behavior of the CH_2 wagging band confirms the assignment, proposed by 2D analysis, of the 1235 cm^{-1} component to the DCE in the clathrate phase. In agreement with the present results, it has been shown that, in the case of s-PS gels, the DCE included in the crystalline nanocavities gives rise to a peak close to 1235 cm^{-1}.[23n]

The asynchronous cross-correlation spectrum of Figure 4 shows two more cross-peaks at [1277, 1235 (−) cm^{-1}] and [1285, 1277 (+) cm^{-1}]. The first peak reflects a host−guest asynchronous correlation, its negative sign indicating a faster dynamic response of the guest feature (trans conformer at 1235 cm^{-1}) with respect to that of the host (at 1277 cm^{-1}). This result is not surprising in view of the much higher molecular mobility of DCE compared to s-PS. The second host−guest asynchronous correlation at [1285, 1277 (+) cm^{-1}] confirms the above temporal relationship for the gauche conformer.

995−820 cm^{-1} Interval. The sequence of spectra collected during the isothermal desorption experiment is displayed in Figure 6 in the region 995−820 cm^{-1}. In this interval all the peaks are associated with the polymeric substrate (except a low intensity absorption at 881 cm^{-1}), making it possible to analyze in detail the evolution of structural order with time. The normal modes in this range are associated with the various out-of-plane hydrogen deformations and follow group frequency correlations developed for monosubstituted benzene derivatives.[37b] The only exception is represented by the peak at 941 cm^{-1} which has been tentatively assigned to a combination tone (406 + 538.9 = 944.9). The overall appearance of the 1D spectra points to an

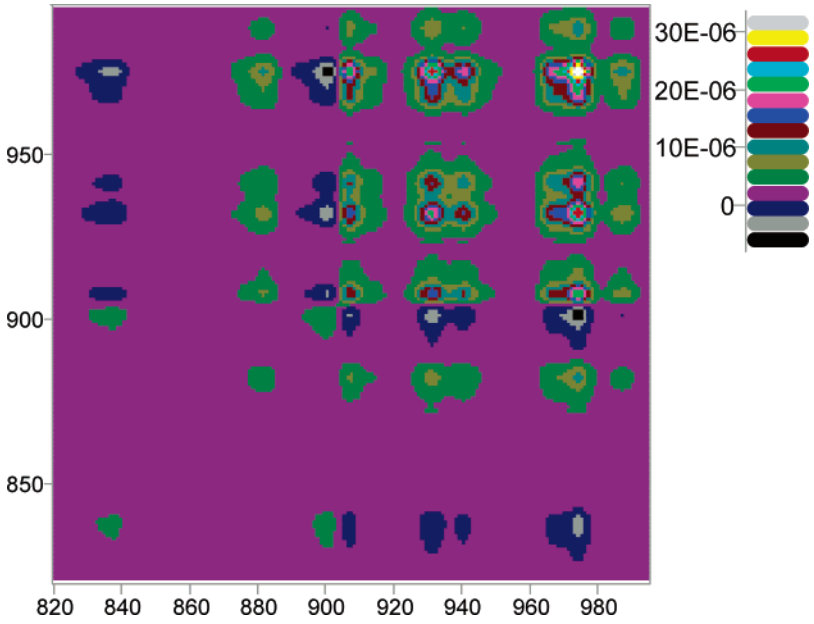

Figure 7. Synchronous 2D correlation spectrum in the wavenumber range 995−820 cm^{-1}.

intensity decrease of all peaks. However, as it will be discussed later, 2D analysis will reveal that this is not the case.

Figure 7 displays the synchronous spectrum obtained from the data of Figure 6; the autopeaks are located at [838, 838 cm^{-1}], [882, 882 cm^{-1}], [901, 901 cm^{-1}], [907, 907 cm^{-1}], [932, 932 cm^{-1}], [941, 941 cm^{-1}], and [975, 975 cm^{-1}] with a well-defined shoulder at [968, 968 cm^{-1}] and another at [988, 988 cm^{-1}].

With respect to the 1D counterparts, the synchronous spectrum reveals the two component structure of the 906 cm^{-1} feature and clearly identifies a minor component at 988 cm^{-1} superimposed on the main absorption at 975 cm^{-1}.

All the above autopeaks display the cross-correlation features at their respective positions; the sign of the cross-peaks is always positive except for those involving the 838 and 901 cm^{-1} autopeaks ([907, 901 (−) cm^{-1}], [932, 901 (−) cm^{-1}], [941, 901 (−) cm^{-1}], [975, 901 (−) cm^{-1}], [907, 838 (−) cm^{-1}], [932, 838 (−) cm^{-1}], [941, 838 (−) cm^{-1}], and [975, 838 (−) cm^{-1}].

Recalling that the negative sign of a cross-peak reflects changes in the opposite direction of the signals involved, we are in the position to assign both the 838 and 901 cm^{-1} components to the amorphous phase, while all the other changing features belong to the crystalline phase. As expected, the synchronous peak correlating the two amorphous signals is positive, since both signals increase. It is explicitly noted that the 1D spectrum of amorphous s-PS displays a peak at 906 cm^{-1} which shifts to 905 cm^{-1} upon heating at 80 °C. Thus, while the synchronous spectrum is able to clearly detect the two component structure of the 906 cm^{-1} band, it underestimates the position of the low frequency component. The reason for this is unclear at present. One possibility may be the occurrence of secondary effects concurrently with the intensity changes, which complicates the overall pattern.

The asynchronous spectrum in Figure 8 shows an intense correlation at [907, 905 (+) cm^{-1}] which is related to the synchronous peak at [907, 901 (−) cm^{-1}]. In this case the position of the low frequency component is in full agreement with the one in the 1D spectrum, possibly because of the resolution enhancement intrinsic in the asynchronous spectrum in comparison to the synchronous one. The occurrence of a slight shift of the two components during the experiment, concurrently with the intensity variation is supported by the characteristic "butterfly shape" of the correlation doublet.[33,41]

A further relevant correlation is identified at [934, 931 (−) cm^{-1}], which reveals the two component structure of the absorption peak at 933 cm^{-1}, with the high frequency feature changing at a slower rate than that at the lower frequency. Also clearly discernible is the cross-peak at [941, 931 (+) cm^{-1}], correlating the two signals appearing at 933 and 941 cm^{-1} in the 1D spectra of Figure 6. Conversely, the two peaks centered at 976 and 967 cm^{-1} in the 1D spectra, while producing an intense synchronous cross-correlation maximum, do not give rise to any feature in the asynchronous spectrum. This result indicates that these two signals are changing at exactly the same rate and, therefore, they display an opposite behavior in comparison to the peaks at 941 and 933 cm^{-1}, although all these features are associated with the crystalline phase. When one is considering crystalline bands, a distinction is to be made between true crystallinity bands due to the crystal force field which manifests itself as a splitting of a single peak into two components, and regularity peaks associated with stereoregular chain segments of variable length, present, to a reasonable approximation, only in the crystalline phase.[40] Although both features can be quantitatively related to the crystallinity degree, their dynamic behavior (as a function of temperature, for instance) is expected to be different. In fact, if a doublet arises as a consequence of crystal field splitting, the two components will disappear concurrently as the crystallinity decreases; conversely, if two peaks are associated with conformational sequences of different length they may show different dynamic response as a function of the external variable. On the basis of the considerations discussed so far the doublet at 976−967 cm^{-1} is tentatively classified as a crystal field splitting, while the three component structure at 941, 934, and 931 cm^{-1} is ascribed to conformationally sensitive, local order bands. This conclusion is supported by the observation

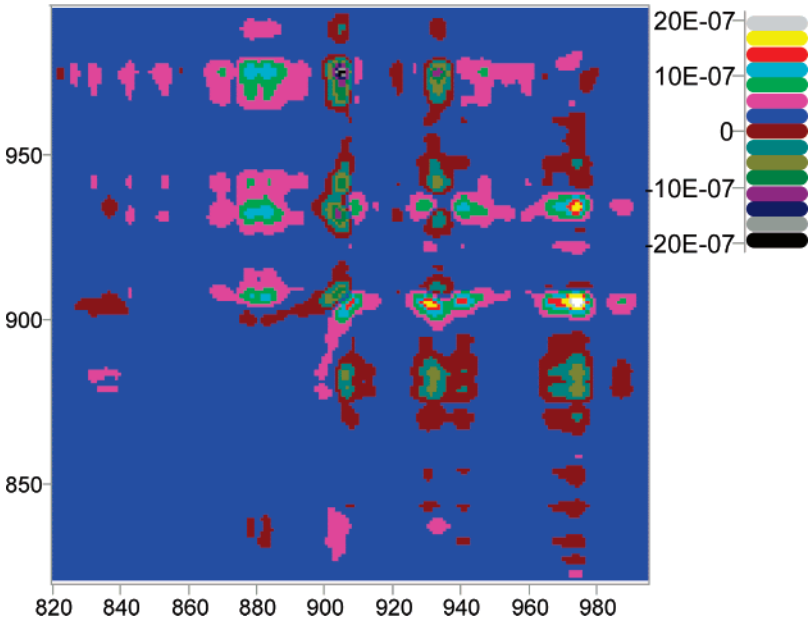

Figure 8. Asynchronous 2D correlation spectrum in the wavenumber range 995−820 cm^{-1}.

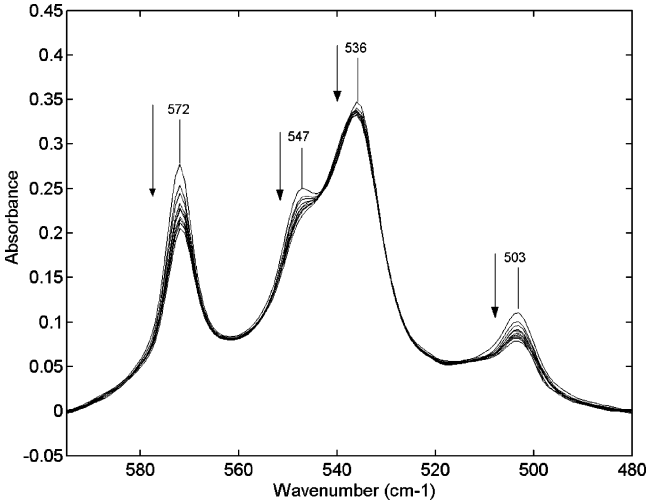

Figure 9. Transmission FTIR spectra in the wavenumber range 595−480 cm^{-1}, collected every 120 min, from 60 to 1200 min, during the isothermal desorption experiment at 80 °C. The arrow's direction indicates absorbance increase or decrease of the corresponding peaks.

that the helical mesomorphic form still displays bands at 941 and 934 cm^{-1}.[12]

595−480 cm^{-1} Interval. In Figure 9 are displayed the FTIR transmission spectra collected at different times during the isothermal desorption experiment at 80 °C. As in the previous frequency range, all the peaks in the present interval are associated with the s-PS spectrum and, in particular, with out-of-plane ring deformation modes.[37b]

The overall appearance of the 1D spectra resembles that already discussed for the 995−870 cm^{-1} interval, in that all the peaks apparently decrease in intensity. However, the synchronous cross-correlation spectrum (see Figure 10) displays negative cross-peaks which point to the presence of an increasing component undetectable in the corresponding 1D spectra. In particular, five autopeaks are observed at [503, 503 cm^{-1}], [534, 534 cm^{-1}], [539, 539 cm^{-1}], [548, 548 cm^{-1}], and [572, 572 cm^{-1}], along with all the cross-peaks at the respective positions. Thus, the enhanced resolution brought about by 2D analysis reveals that the 536 cm^{-1} absorption has, in fact, a two component structure. Furthermore, the cross-peaks originating from the correlation with the component at 539 cm^{-1} (i.e., [539, 503 (−) cm^{-1}], [548, 539 (−) cm^{-1}], and [572, 539 (−) cm^{-1}]) are the only negative features of the synchronous spectrum, which means that the 539 cm^{-1} absorbance peak is the only increasing signal and is therefore related to the amorphous phase, while all the others are associated with the crystalline phase.

The asynchronous cross-correlation spectrum (see Figure 11) displays a peak at [539, 535 (+) cm^{-1}] originating from the two components already detected in the synchronous spectrum. According to the sign of the asynchronous spectrum, the rate of change of the 535 cm^{-1} component is higher than the rate of change of the 539 cm^{-1} component. This conclusion is supported by the sign of the cross-peaks at [537, 503 (+) cm^{-1}] (537 cm^{-1} slower than 503 cm^{-1}, since the corresponding synchronous value is negative) and [548, 537 (−) cm^{-1}] (as above, 537 cm^{-1} slower than 548 cm^{-1}), both confirming the slower evolution of the amorphous feature. The latter is slightly shifted in these two cases to 537 cm^{-1} due to the flatness of the cross-correlation features, which prevents an unambiguous determination of their true positions. In the present system, this result has general validity, in the sense that all the absorbance peaks assigned to the amorphous phase change at a slower rate than the crystalline features with which they are correlated. A physical picture to rationalize this behavior would correspond to a system where the crystalline phase does not directly transform into a fully amorphous phase but passes through an intermediate structure before complete disordering. As a matter of fact, the occurrence of a mesomorphic helical form, characterized by low levels of structural order, has been evidenced by WAXS analysis.[12]

A further important feature revealed by the asynchronous cross-correlation spectrum is the presence of more than one component in the signal at 503 cm^{-1}: cross-correlation peaks are in fact apparent at [503, 496 (−) cm^{-1}] and [509, 503 (+) cm^{-1}] (see Figure 11). The signs of these peaks indicate that both the components

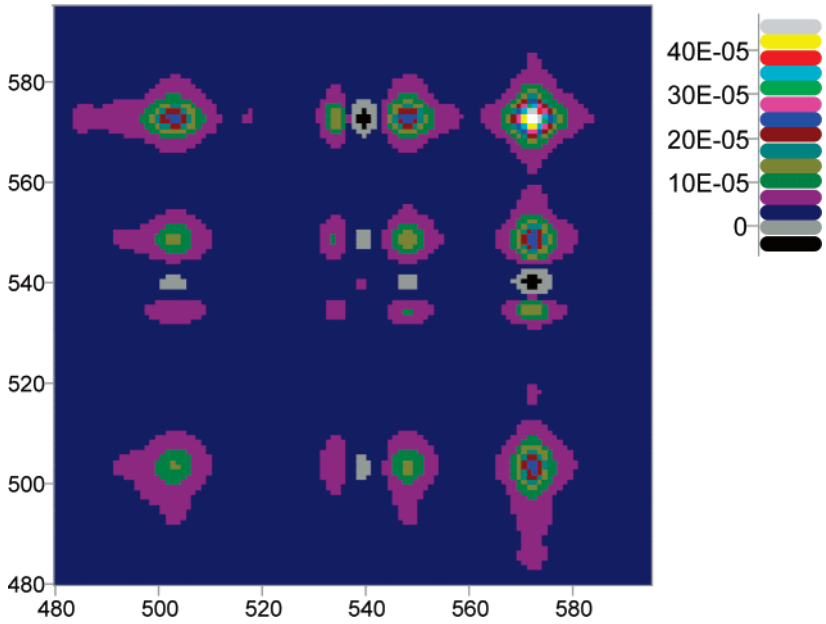

Figure 10. Synchronous 2D correlation spectrum in the wavenumber range 595−480 cm^{-1}.

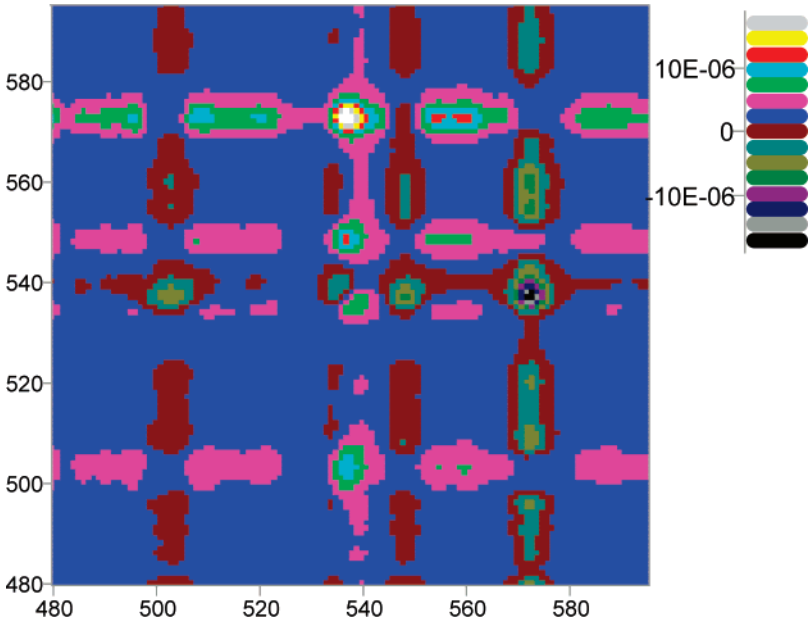

Figure 11. Asynchronous 2D correlation spectrum in the wavenumber range 595−480 cm^{-1}.

at 496, and 509 cm^{-1} change at a faster rate than that at 503 cm^{-1}, which allows us to assign both of them to the crystalline phase. The peaks at 496 and 509 cm^{-1} are asynchronously correlated to the peak at 571 cm^{-1} (i.e., at [496, 571 (−) cm^{-1}] and [509, 571 (−) cm^{-1}]) while no asynchronous correlation is observed between the signals at 571, 548, 533, and 503 cm^{-1}, which give rise to well-defined maxima in the synchronous spectrum.

Analogously, cross-peaks at [571, 555 (−) cm^{-1}] and [571, 560 (−) cm^{-1}] reveal the presence of two components at 560 and 555 cm^{-1} undetected in the 1D spectrum and the negative sign of the asynchronous indicates their crystalline origin.

The 480−600 cm^{-1} region is very sensitive to the overall structural order as well as to the local conformation of the macromolecules;[42] in fact, all the bands appearing in this frequency range display a pronounced dichroic behavior (see Figure 12). According to the literature, the peaks at 571, 548, 533, and 503 cm^{-1} have been assigned to TTGG sequences of different critical sequence length (CSL).[43,44] We recall that CSL is defined as the shorter length of the sequence of a particular conformation, represented by the number m of monomeric units contained in the sequence, necessary for the band to appear. Tashiro et al.[45] using an isotope dilution technique, determined the CSL of the above bands, which is equal to 20−30, 5−10, 7−12, and 12−20 for the absorbance peaks at 571, 548, 533, and 503 cm^{-1}, respectively.

Our results indicate that the experimental profile is considerably more complex than previously reported, with at least nine components in place of the previously reported four.

Furthermore, the sinchronicity of 571, 548, 533, and 503 cm^{-1} peaks could be interpreted assuming that the disordering takes place at the same rate irrespective of the initial sequence length of the chains involved.

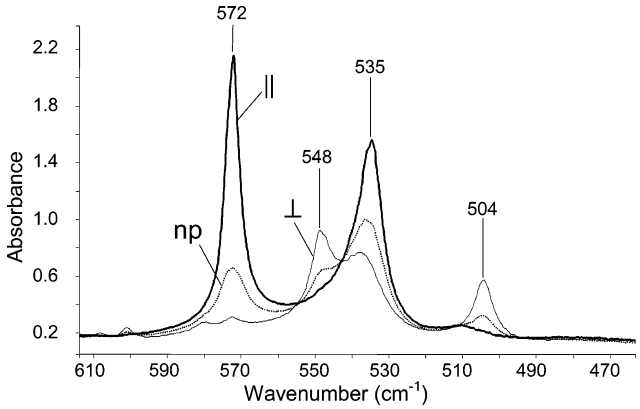

Figure 12. FTIR spectrum in the wavenumber range 610−470 cm^{-1}, collected at resolution of 0.5 cm^{-1} with polarization plane parallel (||) and perpendicular (⊥) to the draw direction, for an uniaxially oriented film ($\lambda \approx 3$) including the s-PS/DCE clathrate phase. The FTIR spectrum of the same uniaxially oriented film collected with unpolarized light at the same resolution (*np*) is also reported for comparison.

Alternatively, the results may be explained assuming that the difference, in terms of CSL between the peaks, is much lower than that reported in the literature, possibly within few monomeric units.

In the present wavenumber range, we do observe asynchronous correlations for a number of components. The asynchronicity produced by the amorphous peak is expected; less obvious are the asynchronous cross-peaks deriving from the crystalline components at 503 and 572 cm^{-1} with those at 496 and 509 cm^{-1}. The above asynchronous features probably reflect a different vibrational origin among the components which are not necessarily associated with specific sequences lengths.

Concluding Remarks

In the present contribution two-dimensional correlation spectroscopy has been applied to analyze the behavior of a clathrate system based on s-PS and DCE. The results obtained demonstrate the usefulness of the present approach for highlighting subtle spectroscopic effects due to host−guest interactions and for interpreting the structural evolution of the system as a consequence of guest desorption. In particular, the following conclusions have been drawn:

(i) A characteristic peak of the guest molecules, i.e., the CH_2 wagging mode of the trans conformer at 1235 cm^{-1}, is significantly influenced by host−guest interactions taking place within the cavity of the s-PS clathrate. This effect is well revealed by 2D IR analysis of the spectral data and is confirmed by high-resolution measurements of axially oriented samples.

(ii) In agreement with previous investigations, the desorption of DCE initially present in the amorphous phase of the sample occurs at a faster rate than the desorption of DCE included into the cavities of the crystalline phase. This effect, in turn, allows us to discriminate between the peaks of DCE absorbed in the two phases.

(iii) With respect to the host s-PS spectrum, it has been evidenced that, in general, the experimental profiles are more complex (i.e., have more unresolved components) than is apparent from a visual inspection of the experimental band shape. Furthermore, several peaks of the amorphous phase have been identified, which were not previously reported.

(iv) In terms of dynamic behavior, it has been found that DCE peaks respond faster to the applied perturbation than the polymer peaks, and within the polymeric substrate, the crystalline phase responds faster than the amorphous phase. The latter effect has been tentatively attributed to the occurrence of a mesomorphic phase.

(v) The 2D-IR analysis of the conformationally sensitive 595−480 cm^{-1} range has evidenced the response synchronicity of the peaks attributed to different CSL's (critical sequences lengths); this interesting effect has been tentatively attributed to a rate of disordering unaffected by the initial sequence length.

Acknowledgment. Financial support of the "Ministero dell'Istruzione, del'Università e della Ricerca" (Prin 2002, Firb2001 and Cluster 26) and of Regione Campania (Legge 5 and Centro di Competenza) is gratefully acknowledged. Thanks are due to Dr. A. Albunia and Mr. G. Orefice for sample preparation and technical assistance in the spectroscopic measurements.

References and Notes

(1) Guerra, G.; Vitagliano, V. M.; De Rosa, C.; Petraccone, V.; Corradini, P. *Macromolecules* **1990**, *23*, 1539.
(2) Chatani, Y.; Shimane, Y.; Inoue, Y.; Inagaki, T.; Ishioka, T.; Ijitsu, T.; Yukinari, T. *Polymer* **1992**, *33*, 488.
(3) De Rosa, C.; Guerra, G.; Petraccone, V.; Corradini, P. *Polym. J.* **1991**, *23*, 1435.
(4) De Rosa, C. *Macromolecules* **1996**, *29*, 8460.
(5) Cartier, L.; Okihara, T.; Lotz, B. *Macromolecules* **1998**, *31*, 3303.
(6) De Rosa, C.; Rapacciuolo, M.; Guerra, G.; Petraccone, V.; Corradini, P. *Polymer* **1992**, *33*, 1423.
(7) De Rosa, C.; Guerra, G.; Corradini, P. *Rend. Fis. Acc. Lincei* **1991**, *2*, 227.
(8) Chatani, Y.; Shimane, Y.; Ijitsu, T.; Yukinari, T. *Polymer* **1993**, *34*, 1625.
(9) De Candia, F.; Filho, A. R.; Vittoria, V. *Makromol. Chem. Rapid Commun.* **1991**, *12*, 295.
(10) Petraccone, V.; Auriemma, F.; Dal Poggetto, F.; De Rosa, C.; Guerra, G.; Corradini, P. *Makromol. Chem.* **1993**, *194*, 1335.
(11) Auriemma, F.; Petraccone, V.; Dal Poggetto, F.; De Rosa, C.; Guerra, G.; Manfredi, C.; Corradini, P. *Macromolecules* **1993**, *26*, 3772.
(12) Manfredi, C.; De Rosa, C.; Guerra, G.; Rapacciuolo, M.; Auriemma, F.; Corradini, P. *Makromol. Chem. Phys.* **1995**, *196*, 2795.
(13) De Rosa, C.; Guerra, G.; Petraccone, V.; Pirozzi, B. *Macromolecules* **1997**, *30*, 4147.
(14) Milano, G.; Venditto, V.; Guerra, G.; Cavallo, L.; Ciambelli, P.; Sannino, D. *Chem. Mater.* **2001**, *13*, 1506.
(15) Chatani, Y.; Shimane, Y.; Inagaki, T.; Ijitsu, T.; Yukinari, T.; Shikuma, H. *Polymer* **1993**, *34*, 1620.
(16) Chatani, Y.; Inagaki, T.; Shimane, Y.; Shikuma, H. *Polymer* **1993**, *34*, 4841.
(17) (a) De Rosa, C.; Rizzo, P.; Ruiz de Ballesteros, O.; Petraccone, V.; Guerra, G. *Polymer* **1999**, *40*, 2103. (b) De Rosa, C.; Rizzo, P.; Ruiz de Ballesteros, O.; Petraccone, V.; Guerra, G. *Polymer* **1999**, *40*, 3895.
(18) Manfredi, C.; Del Nobile, M. A.; Mensitieri, G.; Guerra, G.; Rapacciuolo, M. *J. Polym. Sci., Polym. Phys. Ed.* **1997**, *35*, 133.
(19) Guerra, G.; Milano, G.; Venditto, V.; Musto, P.; De Rosa, C.; Cavallo, L. *Chem. Mater.* **2000**, *12*, 363.
(20) Mensitieri, G.; Venditto, V.; Guerra, G. *Sens. Actuators B* **2003**, *92*, 255.
(21) Yoshioka, A.; Tashiro, K. *Macromolecules* **2003**, *36*, 3001.
(22) Musto, P.; Mensitieri, G.; Cotugno, S.; Guerra, G.; Venditto, V. *Macromolecules* **2002**, *35*, 2296.
(23) (a) Kobayashi, M.; Nakaoki, T.; Ishihara, N. *Macromolecules* **2000**, *23*, 78. (b) Guerra, G.; Musto, P.; Karasz, F. E.; Macknight, W. J. *Makromol. Chem.* **1990**, *191*, 2111. (c) Vittoria, V. *Polym. Commun.* **1990**, *31*, 263. (d) Gowd, E. B.; Nair, S. S.; Ramesh, C. *Macromolecules* **2002**, *35*, 8509. (e) Gowd, E. B.; Nair, S. S.; Ramesh, C.; Tashiro, K. *Macromolecules* **2003**, *36*, 7388. (f) Sivakumar, M.; Yamamoto, Y.; Amutharani, D.; Tsujita, Y.; Yoshimizu, H.; Kinoshita, T. *Macromol. Rapid Commun.* **2002**, *23*, 77. (g) Saitoh, A.;

Amutharani, D.; Yamamoto, Y.; Tsujita, Y.; Yoshimizu, H. *Desalination* **2002**, *148*, 353. (h) Yamamoto, Y.; Kishi, M.; Amutharani, D.; Sivakumar, M.; Tsujita, Y.; Yoshimizu, H. *Polym. J.* **2003**, *35*, 465. (i) Tamai, Y.; Fukuda, M *Chem. Phys. Lett.* **2003**, *371*, 620. (l) Musto, P.; Manzari, M.; Guerra, G. *Macromolecules* **2000**, *33*, 143. (m) Musto, P.; Manzari, M.; Guerra, G. *Macromolecules* **1999**, *32*, 2770. (n) Daniel, C.; Alfano, D.; Guerra, G.; Musto, P. *Macromolecules* **2003**, *36*, 5742.

(24) (a) Noda, I. *Bull. Am. Phys. Soc.* **1986**, *31*, 520. (b) Noda, I. *Bull. Am. Chem. Soc.* **1989**, *111*, 8116. (c) Noda, I. *Appl. Spectrosc.* **1990**, *44*, 550. (d) Noda, I. *Appl. Spectrosc.* **1993**, *47*, 1329.

(25) Meier, R. J.; Steeman P. A. M. *Appl. Spectrosc.* **2002**, *56*, 401.

(26) Noda, I. *Appl. Spectrosc.* **2002**, *56*, 404.

(27) Czarnecki, M. A. *Appl. Spectrosc.* **1998**, *52*, 1583.

(28) Bendat, J. S.; Piersol, A. G. *Engineering Applications of Correlaction and Spectral Analysis*, 2nd ed.; John Wiley and Sons: New York, 1993.

(29) Ekgasit, S.; Ishida, H. *Appl. Spectrosc.* **1995**, *49*, 1243.

(30) Noda, I.; Dowrey, A. E.; Marcott, C. *Appl. Spectrosc.* **1993**, *47*, 1317.

(31) Noda, I.; Dowrey, A. E.; Marcott, C.; Story, G. M.; Ozaki, Y. *Appl. Spectrosc.* **2000**, *54*, 236A.

(32) Zambelli, A.; Longo, P.; Pellecchia, C.; Grassi, A. *Macromolecules* **1987**, *20*, 2035.

(33) Czarnecki, M. A. *Appl. Spectrosc.* **1998**, *52*, 1583.

(34) Czarnecki, M. A. *Appl. Spectrosc.* **1999**, *53*, 1392.

(35) Noda, I. *Appl. Spectrosc.* **2000**, *54*, 994.

(36) (a) Tanabe, K. *Spectrochim. Acta* **1974**, *30A*, 1901. (b) Tanabe, K.; *Spectrochim. Acta* **1972**, *28A*, 407.

(37) (a) Reynolds, N. M.; Hsu, S. L. *Macromolecules* **1990**, *23*, 3463. (b) Nyquist, R. A.; Putzig, C. L.; Leugers, M. A.; McLachlan, R. D.; Thill, B.; *Appl. Spectrosc.* **1992**, *46*, 981.

(38) Guerra, G.; Manfredi, C.; Musto, P.; Tavone, S. *Macromolecules* **1998**, *31*, 1329.

(39) Albunia, A. R.; Di Masi, S.; Rizzo, P.; Milano, G.; Musto, P.; Guerra, G. *Macromolecules* **2003**, *36*, 8695.

(40) Bower, D. I.; Maddams, W. F. *The Vibrational Spectroscopy of Polymers*; Cambridge, England, 1989.

(41) Czarnecki, M. A. *Appl. Spectrosc.* **2000**, *54*, 986.

(42) Liang, C. Y.; Krimm, S. *J. Polym. Sci.* **1958**, *27*, 241.

(43) Kobayashi, M.; Tsumura, K.; Tadokoro, H. *J. Polym. Sci., Polym. Phys. Ed.* **1968**, *6*, 1493.

(44) Kobayashi, M.; Akita, K.; Tadokoro, H. *Makromol. Chem.* **1968**, *113*, 324.

(45) Tashiro, K.; Ueno, Y.; Yoshioka, A.; Kobayashi, M. *Macromolecules* **2001**, *34*, 310.

MA0477899